

Defending Unauthorized Model Merging via Dual-Stage Weight Protection

Wei-Jia Chen¹ Min-Yan Tsai¹ Cheng-Yi Lee² Chia-Mu Yu¹

¹ National Yang Ming Chiao Tung University

² Academia Sinica

{wer9u623, chengyi.lee.1224, chiamuyu}@gmail.com

Abstract

The rapid proliferation of pretrained models and open repositories has made model merging a convenient yet risky practice, allowing free-riders to combine fine-tuned models into a new multi-capability model without authorization. Such unauthorized model merging not only violates intellectual property rights but also undermines model ownership and accountability. To address this issue, we present *MERGE-GUARD*, a proactive dual-stage weight protection framework that disrupts merging compatibility while maintaining task fidelity. In the first stage, we redistribute task-relevant information across layers via L_2 -regularized optimization, ensuring that important gradients are evenly dispersed. In the second stage, we inject structured perturbations to misalign task subspaces, breaking curvature compatibility in the loss landscape. Together, these stages reshape the model’s parameter geometry such that merged models collapse into destructive interference while the protected model remains fully functional. Extensive experiments on both vision (ViT-L-14) and language (Llama2, Gemma2, Mistral) models demonstrate that *MERGE-GUARD* reduces merged model accuracy by up to 90% with less than 1.5% performance loss on the protected model.

1. Introduction

The pretrain–finetune paradigm has become a cornerstone of modern AI, where large pretrained models are efficiently adapted to downstream domains through lightweight finetuning. This workflow, widely adopted in vision [11], language [1, 33], and multimodal [28] communities, has been further catalyzed by open repositories such as Hugging Face [39], GitHub [13], and ModelScope [25], which host thousands of publicly available checkpoints. Developers can now easily obtain and recombine high-quality models without additional training. Among these techniques, model merging [44], which integrates multiple finetuned models derived from the same pretrained source via parameter-level composition, has become a practical means to construct

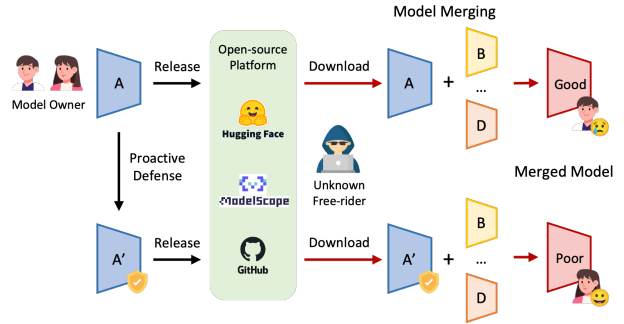


Figure 1. Unauthorized model merging and its defense.

multi-task or cross-domain models [45].

However, this openness also introduces a growing intellectual property risk [9, 43]. Free-riders can download fine-tuned models released under specific license terms and merge them to create new multi-capability models for redistribution or commercial use without authorization. Because parameter blending inherently conceals the provenance of individual weights, such *unauthorized model merging* [18] allows the resulting model to inherit specialized capabilities without reproducing the original training cost or respecting licensing restrictions, posing significant challenges to model ownership [35] and attribution [21].

To mitigate this threat, we propose a *proactive defense* that preprocesses the model’s parameters so that any subsequent merging will degrade functionality while preserving the model’s own task performance. Designing such a defense, however, faces two key challenges. First, the defender can only modify the parameters of their own model and cannot anticipate the attacker’s model, merging strategy, or target tasks, making the defense highly uncertain. Second, the defender must simultaneously maintain the model’s original accuracy and suppress the merged model’s effectiveness under the constraint of controlling only their own parameters (see Figure 1).

We make an observation that recent advances [16, 40, 42, 48] in model merging often rely on sparsification [27, 47], which aims to distribute task-specific information across

different layers and weights before merging. By sparsifying each fine-tuned model, their task-relevant parameters become less overlapping in the parameter space, reducing interference when the two models are later combined. Consequently, the merged model can largely retain the capabilities of each constituent model.

Building on the above observation, we introduce a defensive two-stage preprocessing strategy, MERGEGUARD, to disrupt unauthorized model merging. The key idea is to reshape the model’s weight distribution so that merging no longer preserves task performance. Specifically, we first *re-distribute* the parameter values, spreading those originally concentrated in a few high-magnitude weights across a wider set of parameters. This dispersal maintains the model’s functionality on its original task but makes the merging process unstable, as the diffused weights are more easily amplified, diluted, or interfered with during parameter blending. However, simple averaging alone cannot fully resist merging. To further reinforce protection, we selectively adjust influential parameters by applying controlled perturbations. Because task-relevant knowledge has already been dispersed across many smaller weights, this targeted manipulation minimally affects the standalone model but substantially degrades the performance of any merged version. Through this dual adjustment, MERGEGUARD effectively preserves the integrity of the protected model while inducing collapse in unauthorized merged models.

To validate the robustness of MERGEGUARD, we consider two adaptive attacks. The first attempts to neutralize the defense by subtracting a scaled copy of the protected model’s parameters from the merged weights. The second aims to estimate the hidden disturbance vector and project each gradient update orthogonally to it, avoiding movement along the defended direction during retraining. However, both strategies fail to undermine our defense (see Section 7).

MERGEGUARD has shown high effectiveness on a variety of tasks and architectures. For ViT-L-14 on the GTSRB and MNIST, the accuracy of the preprocessed model only decreased slightly (less than 1%). However, after merging, the accuracy of GTSRB plummeted from 86.78% to 12.19%, and MNIST from 96.02% to 11.35%. For large language models (LLMs), the accuracy after merging generally dropped to single digits, with some even falling to 0%. For example, the accuracy of the Gemma2 decreased from 69.6% to 1.52% on the GSM8K after merging, and from 64.02% to 21.34% on the HumanEval.

Contributions. Our contributions are shown below:

- We propose MERGEGUARD, a proactive defense that redistributes and perturbs model weights to prevent unauthorized merging while preserving task performance.
- Experiments on ViT-L-14, Llama2, Gemma2, and Mistral show that MERGEGUARD reduces merged-model accuracy by up to 90% with less than 1.5% loss

on the protected model.

- We evaluate two adaptive attacks and show that both fail to circumvent the defense due to dispersed task information and unobservable perturbations.

2. Related Works

Model Merging. Model merging is a training-free method for combining multiple fine-tuned models into a single multi-task model by directly manipulating their parameters. Through techniques such as weight averaging (WA) [40], the parameters of several models can be linearly combined to produce a new model capable of handling multiple tasks simultaneously. Task arithmetic (TA) [16] further interprets tasks as vectors in the parameter space, enabling addition or subtraction between task representations. Other approaches, including TIES [4] and DARE [48], enhance merging quality via parameter sparsity and sign consistency, achieving better interpretability without additional data. More recent studies [6, 10, 12, 24, 46] extend these ideas to broader architectures and scenarios, developing increasingly flexible and efficient merging strategies.

Defenses against Unauthorized Model Merging. To the best of our knowledge, PaRaMS [18] is the only work that proactively defends against unauthorized model merging. In particular, PaRaMS introduces parameter rearrangement and random multi-head scaling: the former reorders MLP parameters, and the latter randomly scales attention heads while maintaining functional equivalence, thereby pushing the model out of the shared parameter basin and significantly degrading the merged model’s performance by slightly harming the original task accuracy.

3. Background Knowledge on Model Merging

Let θ_{pre} denote the parameters of the pre-trained model, and θ_i the parameters of a fine-tuned model on task \mathcal{D}_i . For n task-specific models $\theta_1, \dots, \theta_n$ derived from the same pre-trained model θ_{pre} , model merging can be formulated as $\theta_{\text{merge}} = \text{Merge}(\theta_{\text{pre}}, \theta_1, \dots, \theta_n)$, where Merge represents a specific parameter-level fusion strategy.

Task Arithmetic (TA). TA [16] assumes that the task-specific update from θ_{pre} to θ_i encodes the distinctive capability of task \mathcal{D}_i . This update, referred to as the *task vector* $\tau_i = \theta_i - \theta_{\text{pre}}$, can be linearly combined across tasks to obtain $\theta_{\text{merge}} = \theta_{\text{pre}} + \lambda \sum_i \tau_i$, where λ controls the merging scale. TA therefore constructs a multi-task model by directly superposing these task vectors.

TIES-Merging. Extending TA, TIES-merging [42] aims to alleviate interference between tasks caused by redundant or conflicting parameters. It first trims each task vector τ_i by retaining only the top- $k\%$ parameters with the largest magnitudes, then elects a unified parameter sign across tasks, and finally performs a disjoint merge that averages only the

parameters consistent with the selected sign. This three-step procedure improves stability and reduces destructive interference in the merged model.

AdaMerging. AdaMerging [46] introduces an adaptive and unsupervised model merging framework that automatically learns task-wise or layer-wise coefficients without using original training data. By minimizing prediction entropy on unlabeled samples, it adjusts merging weights to balance task contributions, thereby improving multi-task performance, generalization, and robustness. This adaptive strategy can be integrated with TA or TIES-merging to further enhance merging quality and stability.

4. System Model

Attack Scenario. We consider a common scenario in which a *defender* fine-tunes a large pretrained model θ_{pre} on a domain-specific dataset to achieve high task performance and subsequently releases the model θ_{def} to the community. A *free-rider*, however, may download this open-sourced model and merge it with another model under their control. We assume that the free-rider’s model, θ_{fr} , is also fine-tuned from the same pretrained model θ_{pre} , a typical setup in current practice since most finetuning pipelines start from public backbones. By merging the two models, the free-rider seeks to inherit the defender’s specialized capabilities at minimal cost and combine them with their own model’s functionality. The defender’s goal is therefore to proactively modify its model θ_{def} so that it remains fully functional on the intended task but loses effectiveness when merged with any other model.

Free-rider’s Capability. The free-rider is assumed to have limited computational resources, making expensive retraining or knowledge distillation [15, 36] infeasible. In particular, because the free-rider is highly cost-sensitive, they will not perform knowledge distillation on T_{def} even though the dataset is downloadable, as such retraining still incurs substantially higher computation and tuning costs than direct parameter merging. Instead, they rely on low-cost model merging as a shortcut to acquire the defender’s expertise. The free-rider has full white-box access to the defender’s released model and a task-specific model θ_{fr} derived from the same θ_{pre} . The attack is considered successful if the merged model θ_{merge} achieves accuracy comparable to θ_{def} on the defender’s task T_{def} while preserving its own performance on T_{fr} , where T_X denotes X ’s domain-specific task.

Defender’s Capability. The defender has full access to and control over the parameters of their own model θ_{def} and can apply parameter-level transformations to strengthen protection. These modifications must maintain the model’s original task performance while preventing the merged model from retaining it. Although the defender cannot access the free-rider’s model, it can reasonably assume both originate from the same model θ_{pre} ; otherwise, merging would not be

feasible [6, 10, 12, 16, 24, 40, 46]. A successful defense ensures that the released model remains fully functional for legitimate use, but any merged version experiences a substantial accuracy drop on T_{def} .

Problem Setup. The free-rider’s goal is to construct a merged model $\theta_{\text{merge}} = \text{Merge}(\theta_{\text{pre}}, \theta_{\text{def}}, \theta_{\text{fr}})$ that simultaneously satisfies $\text{Perf}(\theta_{\text{merge}}, T_{\text{def}}) \approx \text{Perf}(\theta_{\text{def}}, T_{\text{def}})$ and $\text{Perf}(\theta_{\text{merge}}, T_{\text{fr}}) \approx \text{Perf}(\theta_{\text{fr}}, T_{\text{fr}})$, where $\text{Merge}(\cdot)$ denotes a parameter-level fusion method such as model soups or task arithmetic [6, 10, 12, 16, 24, 40, 46], and $\text{Perf}(\cdot)$ represents the appropriate utility metric for the target model family (*e.g.*, accuracy for vision or perplexity for language models). To counter this, the defender instead releases a protected model $\hat{\theta}_{\text{def}} = \text{Defense}(\theta_{\text{def}})$ whose standalone performance remains intact, $\text{Perf}(\hat{\theta}_{\text{def}}, T_{\text{def}}) \approx \text{Perf}(\theta_{\text{def}}, T_{\text{def}})$, but any merged version $\hat{\theta}_{\text{merge}} = \text{Merge}(\theta_{\text{pre}}, \hat{\theta}_{\text{def}}, \theta_{\text{fr}})$ exhibits a pronounced degradation, $\text{Perf}(\hat{\theta}_{\text{merge}}, T_{\text{def}}) \ll \text{Perf}(\theta_{\text{def}}, T_{\text{def}})$. Therefore, our objective is to design a proactive defense function $\text{Defense}(\cdot)$ that enforces this degradation property while maintaining the protected model’s utility on its intended task.

5. Proposed Method

To address unauthorized merging, we propose **MERGE-GUARD**, which comprises two stages: ① *Density-Aware Finetuning* (training stage) and ② *Adversarial Weight Negation* (training-free stage). We first outline the key idea behind **MERGE-GUARD**, then describe each stage in detail.

Key Idea. As discussed in Section 3, most recent model merging techniques, such as TIES [42] and AdaMerging [46] rely on sparsification to distribute task-relevant parameters sparsely across layers, reducing interference and enabling merged models to preserve multiple capabilities.

As shown in Figure 2, **MERGE-GUARD** builds on this observation from a defensive perspective. In the first stage, *Density-Aware Finetuning* disperses task-critical weights through L_2 -regularized training, ensuring that important information is evenly spread across layers rather than concentrated in a few parameters. This dispersed structure provides stability for the second stage, *Adversarial Weight Negation*, which selectively offsets a subset of task-relevant directions to intentionally misalign them with potential merging counterparts. Because the weight importance has already been evenly distributed by *Stage 1*, these perturbations preserve the model’s own task performance while disrupting the cross-model compatibility required for successful merging. Together, the two stages reshape the parameter landscape so that merging attempts result in destructive interference, effectively neutralizing unauthorized model combination.

Stage 1: Density-Aware Finetuning. The goal of this stage is to disperse task-critical weights across different

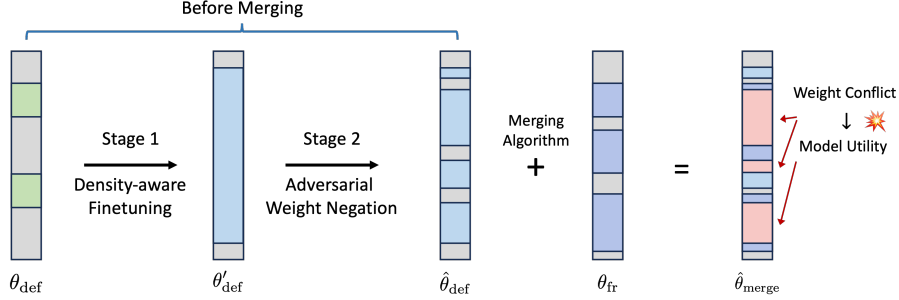


Figure 2. The workflow of MERGE GUARD.

layers through training. In addition to the standard cross-entropy loss L_{CE} used in classification, we introduce an L_2 regularization term that drives model parameters toward zero, encouraging a more balanced distribution of important information. The total loss function is formulated as:

$$L_{\text{Total}} = L_{\text{CE}} + \alpha L_2 \quad (1)$$

Specifically, for vision tasks, the loss can be explicitly expanded as:

$$L_{\text{Total}} = - \sum_{t=1}^T y_t \log(\hat{y}_t) + \alpha \sum_{\ell=1}^L \|\theta^{(\ell)}\|_2^2, \quad (2)$$

where y_t and \hat{y}_t denote the ground-truth label and the predicted probability for the t -th class, respectively; α is a hyperparameter balancing the two terms; and $\theta^{(\ell)}$ represents the trainable parameters of the ℓ -th layer. Crucially, the L_2 penalty is applied layer-wise so that each layer is regularized independently.

Similarly, for LLMs, the objective function is formulated based on next-token prediction:

$$L_{\text{Total}} = - \sum_{t=1}^T \log P(y_t | y_{<t}, x; \theta) + \alpha \sum_{\ell=1}^L \|\theta^{(\ell)}\|_2^2, \quad (3)$$

where $P(y_t | y_{<t}, x; \theta)$ denotes the conditional probability of predicting the token y_t given the preceding context $y_{<t}$ and input x . This formulation applies L_2 regularization across all layer parameters, effectively smoothing large-magnitude weights and promoting an even distribution of task-relevant signals throughout the network layers.

Overall, given θ_{def} , we obtain θ'_{def} after *Stage 1*. By reducing the concentration of dominant weights, this stage effectively disperses important information throughout the model, making subsequent merging operations less stable and thereby diminishing the merged model’s performance.

Stage 2: Adversarial Weight Negation. This stage introduces a training-free procedure that intentionally offsets task-relevant weights to disrupt merging compatibility. We begin by masking each layer of the model and measuring the resulting accuracy drop. The top k' % of layers that cause

the largest performance degradation are identified as critical and excluded from subsequent operations. Afterwards, a binary masking vector M is then constructed, where elements corresponding to k' % critical layers and to the least significant $(1-k)(1-k')$ % parameters are set to zero, and those in the remaining $k(1-k')$ % range are set to one. This selective preservation ensures that later weight adjustments do not damage essential functionality. Next, we calculate

$$\hat{\theta}_{\text{def}} = \theta'_{\text{def}} - \beta M \odot \tau'_{\text{def}}, \quad (4)$$

where \odot denotes the inner product, $\tau'_{\text{def}} = \theta'_{\text{def}} - \theta_{\text{pre}}$ denotes the task vector representing the direction of the defender’s fine-tuning, and $\beta > 0$ is a small perturbation factor. Subtracting τ_{def} in the masked parameter space weakens certain informative directions without compromising the core task performance. Consequently, the protected model remains stable on its own task, but any merged version suffers severe degradation due to misaligned task directions and dilution introduced by the merging algorithm.

We note that some layers differ substantially in parameter scale across tasks, and applying this operation directly can destabilize the model. To prevent collapse in LLMs, we exclude three layers, *model.embed.tokens.weight*, *model.norm.weight*, and *lm.head.weight*, from the subtraction process, while ViT-based models undergo the full operation.

Theoretical Justification of MERGE GUARD. Model merging can be expressed as a parameter-level combination:

$$\theta_{\text{merge}} = \theta_{\text{pre}} + \lambda_1(\theta_{\text{def}} - \theta_{\text{pre}}) + \lambda_2(\theta_{\text{fr}} - \theta_{\text{pre}}), \quad (5)$$

where $\lambda_1, \lambda_2 \in [0, 1]$ control the blending ratio. A successful merge implicitly assumes that both task vectors $\tau_{\text{def}} = \theta_{\text{def}} - \theta_{\text{pre}}$ and $\tau_{\text{fr}} = \theta_{\text{fr}} - \theta_{\text{pre}}$ reside in a *shared linear subspace* representing compatible gradient directions [31, 37, 49]. In this case, their superposition still corresponds to a descent direction in the loss landscape [3, 22], preserving both tasks.

MERGE GUARD breaks this assumption by jointly modifying both the *magnitude distribution* and the *directional*

alignment of τ_{def} . Formally, after *Stage 1*, the finetuned parameters become $\theta'_{\text{def}} = \theta_{\text{pre}} + \tau'_{\text{def}}$, where $\tau'_{\text{def}} = \tau_{\text{def}} + \epsilon$, $\mathbb{E}[\epsilon] = 0$, and $\text{Cov}[\epsilon] = \sigma^2 I$. This step redistributes task-relevant gradients more isotropically, flattening the curvature of the local basin and ensuring that important information is evenly spread rather than concentrated along a few dominant directions. As a result, the Hessian eigenvectors associated with large eigenvalues that previously spanned the shared merging subspace become decorrelated and dispersed.

Then, *Stage 2* injects a small but structured perturbation along a *locally adversarial* direction: $\hat{\theta}_{\text{def}} = \theta'_{\text{def}} - \beta M \odot \tau'_{\text{def}}$ (Eq. 4). This operation effectively rotates the task vector by an angle $\phi = \arccos \frac{\langle \tau'_{\text{def}}, \tau_{\text{fr}} \rangle}{\|\tau'_{\text{def}}\| \|\tau_{\text{fr}}\|}$, thereby increasing the expected interference term in the merged loss:

$$\Delta \mathcal{L}_{\text{merge}} \approx \lambda_1 \lambda_2 \|\tau'_{\text{def}}\| \|\tau_{\text{fr}}\| (1 - \cos \phi), \quad (6)$$

which grows quadratically with the misalignment angle. In practice, even small rotations (e.g., $\phi > 30^\circ$) suffice to push the merged model outside the shared basin, causing the loss landscape to exhibit destructive interference between the two task vectors. As the masked perturbation preserves low-order statistics within each critical layer, the standalone model maintains its original functionality, while any linear or sparsity-based fusion [6, 10, 12, 16, 24, 40, 46, 48] collapses due to incompatible curvature directions.

Hence, MERGE GUARD’s defense can be theoretically interpreted as *inducing curvature misalignment* in the task subspace, transforming the previously compatible manifold of fine-tuned models into disjoint basins. This ensures that the merged parameter θ_{merge} no longer lies near a stationary point of either task’s loss function, leading to substantial degradation in unauthorized merged models.

6. Evaluation

6.1. Experiment Setups

Models. For the image classification task, we adopt the ViT-L-14 [11] architecture, a transformer-based vision backbone widely used for downstream adaptation. For image generation, we employ Stable Diffusion 1.5 (SD1.5) [29], a latent diffusion model trained on large-scale text–image pairs. For the language tasks, we evaluate three representative architectures: Llama2-7B [33], Gemma2-9B [32], and Mistral-7B [17].

Datasets. For image classification, we evaluate across eight diverse datasets: SUN397 [41], Cars [19], RESISC45 [5], SVHN [26], GTSRB [30], MNIST [20], EuroSAT [14], and DTD [7], which span natural scenes, fine-grained objects, digits, satellite imagery, and textures. For image generation, we consider WikiArt [38] and Naruto [2]. For LLM evaluation, we employ AlpacaEval [23] for instruction fol-

lowing, GSM8K [8] for mathematical reasoning, and HumanEval [4] for program synthesis. Details about these datasets are shown in the Appendix.

Metrics. In image classification, we report top-1 accuracy to assess recognition capability. For LLMs, the AlpacaEval benchmark reports the win rate against Zephyr-7B [34]; the GSM8K benchmark measures the proportion of correctly solved problems; and the HumanEval benchmark measures pass@1 accuracy [4], indicating the fraction of valid programs that pass all test cases.

Merging Methods. We assess the robustness of MERGE GUARD under multiple representative model-merging paradigms, including Weight Averaging (WA) [40], Task Arithmetic (TA) [16], TIES-Merging (TIES) [42], and AdaMerging (ADA) [46], with DARE [48] additionally employed as an optional pre-processing module to form DT (DARE+TIES) used in LLMs.

Baselines. Following prior work, PaRaMS [18] serves as the only proactive defense specifically designed against unauthorized model merging. Hence, we use PaRaMS as the sole baseline for quantitative comparison.

Implementation of MERGE GUARD. Our implementation of the *Density-Aware Finetuning* stage requires no additional hyperparameter tuning. The *Adversarial Weight Negation* stage introduces two key hyperparameters: k' and k , which control the proportion of preserved and perturbed layers, respectively. Unless otherwise specified, we set $k' = 10$ and $k = 0.1$ for all experiments. In Eq. 1, we set $\alpha = 0.01$, while β in *Stage 2* is set to 1. Merging coefficients are determined following the protocols of the respective model merging methods [16, 40, 42, 46, 48].

Table 1. Standalone model accuracy before/after MERGE GUARD.

	SUN397	Cars	RESISC45	EuroSAT	SVHN	GTSRB	MNIST	DTD
θ_{pre}	68.24	77.94	71.33	62.72	58.45	50.55	76.36	55.37
θ_{def}	82.32	92.39	97.37	99.81	98.11	99.24	99.69	84.15
$\hat{\theta}_{\text{def}}$	81.52	8829	97.25	95.46	96.82	98.25	99.27	82.16

6.2. Experimental Results

6.2.1. Results on Image Classification

Table 1 summarizes the classification accuracy of θ_{pre} , θ_{def} , and $\hat{\theta}_{\text{def}}$. As expected, fine-tuning θ_{pre} on T_{def} substantially improves performance, confirming the effectiveness of task adaptation. Comparing θ_{def} with $\hat{\theta}_{\text{def}}$, we observe that MERGE GUARD maintains nearly identical accuracy, introducing only a negligible drop, which demonstrates that the protection process preserves the model’s original utility.

Table 2 summarizes the image classification results on MERGE GUARD under different model merging methods. Across all evaluated merging paradigms, MERGE GUARD consistently enforces significant degradation on the merged models while preserving the original model’s performance.

Table 2. Classification accuracy of the merged models without MERGEGuard (θ_{merge}) and with MERGEGuard ($\hat{\theta}_{\text{merge}}$).

Method	SUN397		Cars		RESISC45		EuroSAT		SVHN		GTSRB		MNIST		DTD	
	θ_{merge}	$\hat{\theta}_{\text{merge}}$														
WA [40]	72.1	56.16	81.6	76.63	82.6	4.98	91.9	13.07	78.2	10.05	70.7	44.28	97.1	38.97	62.8	2.61
TA [16]	73.9	54.27	82.1	38.24	86.6	56.50	94.1	54.94	87.9	47.28	86.7	12.91	98.9	11.35	65.6	46.65
TIES [42]	76.5	70.77	85.0	45.64	89.3	33.51	95.7	14.48	90.3	7.77	83.3	4.44	99.0	35.70	68.6	48.88
ADA [46]	79.4	65.51	90.3	74.19	91.6	72.27	97.4	11.22	93.4	7.76	97.5	2.19	99.0	71.37	79.2	49.20

Table 3. The comparison between MERGEGuard and PaRaMS [18]. Each number corresponds to the classification accuracy (%). The average accuracy drop is 30.76 for PaRaMS and is 52.11 for MERGEGuard.

Methods	SUN397		Cars		RESISC45		EuroSAT		SVHN		GTSRB		MNIST		DTD	
	$\hat{\theta}_{\text{def}}$	$\hat{\theta}_{\text{merge}}$														
PaRaMS [18]	82.32	56.77	92.39	38.61	97.37	67.86	99.81	74.81	98.11	71.95	99.24	52.25	99.69	96.02	84.15	48.72
MERGE Guard	81.52	54.27	88.29	38.24	97.25	56.50	95.46	54.94	96.82	47.28	98.25	12.91	99.27	11.35	82.16	46.65

In particular, the preprocessing causes only a marginal reduction (typically less than 1%) in standalone accuracy, indicating that the dual-stage mechanism minimally affects the base model’s functionality. However, once the protected models are merged, their accuracy drops drastically across all datasets. Compared to the unprotected or baseline configurations, MERGEGuard achieves much larger post-merge degradation across all merging strategies.

Table 3 summarizes the image classification results comparing MERGEGuard with PaRaMS [18]. During the preprocessing stage, MERGEGuard introduces a minor accuracy drop on the original model due to the regularization and perturbation applied in the protection process. In contrast, PaRaMS [18], which only performs parameter rearrangement, preserves the original accuracy almost perfectly. However, after model merging, the gap between the two defenses becomes substantial. MERGEGuard consistently enforces stronger degradation on the merged models while maintaining near-original accuracy on the protected model. For instance, on GTSRB and MNIST, MERGEGuard in TA reduced the original accuracy by less than 2%, yet the merged accuracy dropped sharply from 86.78% to 12.91% and from 98.94% to 11.35%, respectively. By comparison, PaRaMS only reduced the same metrics to 52.25% and 96.02%. These results confirm that MERGEGuard substantially weakens merging compatibility.

6.2.2. Results on Image Generation

Figure 3 illustrates the qualitative comparison on SD 1.5. We use Naruto as the defender’s task (T_{def}) and WikiArt as the free-rider’s task (T_{fr}). The first two columns visualize the images generated by θ_{def} and θ_{fr} , respectively. When tested with prompts A_0 and A_1 designed for Naruto, the free-rider’s model θ_{fr} can also reproduce the character, indicating that it has captured the semantic style of Naruto. The merged model θ_{merge} , obtained through standard parameter fusion, inherits this capability and successfully generates

Naruto-style images, demonstrating a clear case of intellectual property leakage.

In contrast, under MERGEGuard, the protected standalone model $\hat{\theta}_{\text{def}}$ maintains its generative fidelity, producing faithful Naruto imagery. However, the protected merged model $\hat{\theta}_{\text{merge}}$ fails to replicate the character, yielding only incoherent or semantically mismatched outputs. This degradation confirms that MERGEGuard effectively prevents the unauthorized inheritance of generative capabilities without compromising the original model’s utility.

6.2.3. Results on Text Classification

Figure 4 illustrates MERGEGuard’s performance across various LLM merging strategies. While protected models maintain competitive accuracy prior to merging, their performance collapses post-merge across all benchmarks. For instance, both Llama2 and Mistral experience nearly a 50% drop in overall accuracy, while Gemma2 suffers even more severe degradation. Notably, on the GSM8K mathematical reasoning benchmark, merged models become virtually nonfunctional, frequently skipping reasoning steps or making elementary calculation errors, with accuracy often plunging to single digits (e.g., Mistral with TA drops from 75.7% to 0%). Similarly, on the HumanEval code generation task, MERGEGuard consistently reduces post-merge pass@1 accuracy by over 50%. Qualitative analysis (see Appendix) further reveals that while some generated programs pass basic test cases, they often contain redundant logic or infinite loops.

6.3. Ablation Studies

To evaluate the contribution of each stage in MERGEGuard, we compare the effects of applying *Stage 1*, *Stage 2*, and their combination (*Stage 1 + 2*). Table 4 reports the performance of the ViT-L/14 across multiple datasets, where it shows baseline accuracy before applying any protection, and presents results after each protection configuration. We ob-

Prompt Example:

A_0 : “A young warrior with a headband stands in a mystical forest filled with soft glowing lights, surrounded by ancient trees and floating spirits, cinematic lighting, painterly style, calm yet powerful atmosphere, detailed background.”

A_1 : “A young fighter performing a wind technique atop a mountain village, swirling leaves around him, sunset sky with warm tones, delicate brushstrokes, nostalgic yet energetic mood, inspired by traditional Japanese scenery.”

B : “A cityscape in the style of Pierre Auguste Renoir”



Figure 3. Visualization Results of SD 1.5.

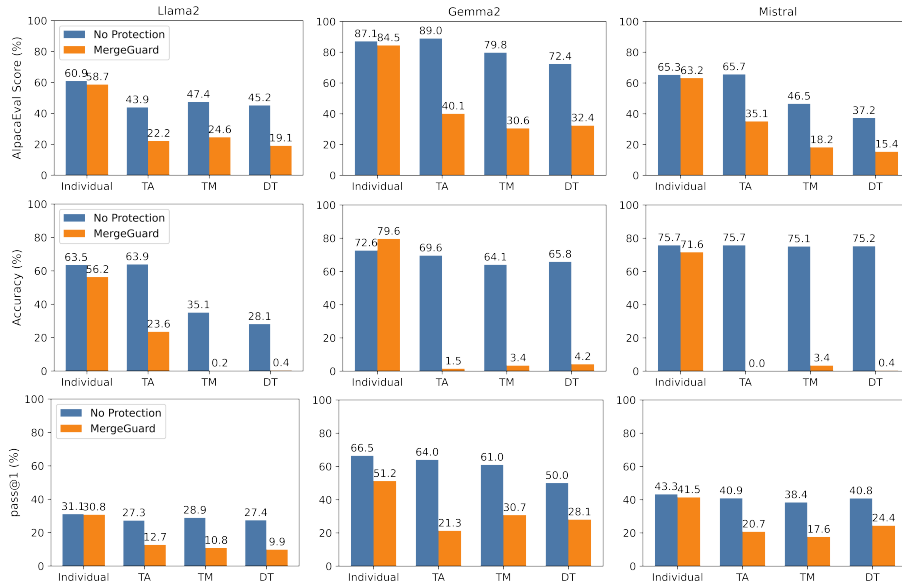


Figure 4. Overall comparison across benchmarks and models. Each row corresponds to a benchmark (AlpacaEval for instruction-following, GSM8K for reasoning, and HumanEval for code generation), and each column corresponds to a model (Llama2, Gemma2, Mistral). Orange and blue bars denote results with and without MERGE GUARD, respectively.

Table 4. The results of the ablation study. Each number indicates classification accuracy (%).

Method	SUN397		Cars		RESISC45		EuroSAT		SVHN		GTSRB		MNIST		DTD	
	$\hat{\theta}_{def}$	$\hat{\theta}_{merge}$														
Stage I	79.96	76.38	90.79	72.25	93.48	85.38	98.07	75.06	97.29	81.21	98.37	12.21	99.30	13.37	81.77	63.60
Stage II	80.10	75.94	92.10	77.33	92.74	75.33	99.83	79.79	98.11	77.88	99.25	64.86	99.73	83.60	80.16	54.20
Stage I + II	79.14	54.27	88.29	38.24	92.16	56.50	95.46	54.94	96.82	47.28	98.25	12.91	99.27	11.35	80.08	46.65

serve that although the standalone stages cause a similar minor accuracy drop before merging, their combination (*Stage 1 + 2*) leads to a much larger degradation in the merged model’s accuracy. This indicates that the two stages complement each other: *Stage 1* disperses task-relevant weights to stabilize the model, while *Stage 2* exploits this dispersed structure to misalign merging directions effectively.

6.4. Discussion

Why MERGE GUARD Outperforms PaRaMS in Image/Text Classification. Compared with PaRaMS, which relies solely on deterministic parameter rearrangement and random multi-head scaling, MERGE GUARD’s two-stage process produces more structured disruption in task-space geometry. In image and text classification, tasks are dominated by discriminative gradients that occupy relatively low-dimensional subspaces. MERGE GUARD’s weight redistribu-

tion amplifies the sensitivity of these subspaces to cross-task interference: the dispersed small weights contribute collectively to stable single-task performance but amplify destructive interference under linear merging, leading to a steeper accuracy collapse than PaRaMS. From a loss landscape perspective [3, 22], MERGEGUARD reshapes each classifier’s basin into multiple narrow valleys separated by sharp ridges, while PaRaMS merely translates the basin position. Thus, the merged model under MERGEGUARD lands closer to the curvature apex (high loss), producing stronger merging degradation.

Why $\hat{\theta}_{\text{merge}}$ Cannot Generate Random Noise. As discussed in Section 6.2.2, the MERGEGUARD-protected merged model $\hat{\theta}_{\text{merge}}$ fails to reproduce the defender’s task T_{def} but does not completely collapse into random noise. In contrast, the PaRaMS-protected merged model often outputs pure noise patterns. Both defenses achieve equivalent levels of intellectual property protection, neither reveals task-specific visual traits from T_{def} , yet the perceptual outcomes differ significantly.

This discrepancy stems from how each method disrupts representational continuity in generative models. Diffusion-based generators depend on smooth manifold alignment between latent and pixel spaces. PaRaMS introduces random multi-head scaling and parameter rearrangement, which destroy such continuity, leading to decorrelated feature channels and a complete breakdown of the generative structure. In contrast, MERGEGUARD perturbs model parameters in a structured manner: its L_2 -regularized redistribution preserves weak weight correlations that maintain partial coherence in the latent manifold. Thus, MERGEGUARD prevents semantic fidelity without inducing total noise collapse.

In essence, PaRaMS enforces representational incoherence across generative layers, while MERGEGUARD enforces functional incompatibility within discriminative subspaces. Hence, PaRaMS is more disruptive for continuous generative pipelines (e.g., diffusion models), whereas MERGEGUARD is better suited for discriminative or classification-oriented tasks where decision-boundary misalignment is the primary defense objective.

7. Adaptive Attack

The free-rider may be aware of the deployment of MERGEGUARD and could develop adaptive attacks to circumvent it. We consider two such adaptive attacks, UNMASK and GRADERASE, described below.

UNMASK. The design rationale behind UNMASK is to neutralize the defensive perturbation introduced by MERGEGUARD by directly subtracting the protected model’s parameters from the merged weights. Specifically, the free-rider constructs an adaptive model $\theta_{\text{Unmask}} = \text{Merge}(\theta_{\text{pre}}, \hat{\theta}_{\text{def}}, \theta_{fr}) - \lambda \cdot \hat{\theta}_{\text{def}}$, where λ follows the scaling factor used in TA (0.3 in our experiments).

Table 5. Evaluation of different adaptive attacks.

	SUN397	Cars	RESISC45	EuroSAT	SVHN	GTSRB	MNIST	DTD	Avg.
θ_{pre}	68.24	77.94	71.33	62.72	58.45	50.55	76.36	55.37	65.12
$\hat{\theta}_{\text{merge}}$	73.90	82.10	86.60	94.10	87.90	86.70	98.90	65.60	84.47
$\hat{\theta}_{\text{merge}}$	54.27	38.24	56.50	54.94	47.28	12.91	11.35	46.65	40.26
UNMASK	67.75	71.19	68.35	64.44	68.71	51.50	71.79	53.46	64.64
GRAD ERASE	67.36	71.58	76.60	64.10	54.08	14.58	10.28	55.60	51.77

GRADERASE. GRADERASE is designed to counteract MERGEGUARD by removing the gradient component aligned with the defender’s hidden perturbation direction. Specifically, the free-rider estimates the disturbance vector $v_{\text{disturb}} = -\tau_G$ from limited training data and modifies each gradient update as $g' = g - \frac{\langle g, v_{\text{disturb}} \rangle}{\|v_{\text{disturb}}\|^2} v_{\text{disturb}}$, thereby eliminating the defensive direction during retraining.

Summary of Adaptive Attacks. For UNMASK, although subtracting the protected model’s parameters can partially neutralize MERGEGUARD’s perturbations, it concurrently removes essential task-specific information, causing the merged model’s performance on T_{def} to regress to the pretrained level T_{pre} , as shown in Table 5. In contrast, GRADERASE projects each gradient update orthogonally to the estimated disturbance vector v_{disturb} to avoid reinforcing the defended direction. However, as the estimation of v_{disturb} is inherently noisy and incomplete, this attack fails to fully restore merging compatibility.

As summarized in Table 5, MERGEGUARD reduces the average merged accuracy from 84.47% to 40.26%. Although adaptive attacks such as Unmask and GradErase can partially recover performance to 64.64% and 51.77% respectively, MERGEGUARD consistently maintains a substantial degradation margin of at least 20% across all tasks. These results demonstrate that even under adversarial settings, MERGEGUARD remains robust, effectively preventing the merged model from regaining functional usability.

8. Conclusion

We presented MERGEGUARD, a dual-stage defense that proactively prevents unauthorized model merging. By redistributing and adversarially perturbing task-relevant weights, MERGEGUARD disrupts curvature alignment in the loss landscape, making merged models collapse while preserving the original task performance. Extensive experiments show up to 90% degradation in merged accuracy with minimal impact on the protected model. Compared to PaRaMS, MERGEGUARD achieves stronger resistance in discriminative tasks, revealing that shaping weight geometry, not just rearranging parameters, is key to safeguarding model ownership.

References

- [1] Tom Brown, Benjamin Mann, Nick Ryder, Melanie Subbiah, Jared D Kaplan, Prafulla Dhariwal, Arvind Neelakantan, Pranav Shyam, Girish Sastry, Amanda Askell, et al. Language models are few-shot learners. *NeurIPS*, 33:1877–1901, 2020. 1
- [2] Eole Cervenka. Naruto blip captions. <https://huggingface.co/datasets/lambdalabs/naruto-blip-captions/>, 2022. Accessed: 2025-11-12. 5, 1
- [3] Huanran Chen, Yinpeng Dong, Zeming Wei, Yao Huang, Yichi Zhang, Hang Su, and Jun Zhu. Unveiling the basin-like loss landscape in large language models. *arXiv preprint arXiv:2505.17646*, 2025. 4, 8
- [4] Mark Chen. Evaluating large language models trained on code. *arXiv preprint arXiv:2107.03374*, 2021. 2, 5, 1
- [5] Gong Cheng, Junwei Han, and Xiaoqiang Lu. Remote sensing image scene classification: Benchmark and state of the art. *Proceedings of the IEEE*, 105(10):1865–1883, 2017. 5, 1
- [6] Jiho Choi, Donggyun Kim, Chanhyuk Lee, and Seunghoon Hong. Revisiting weight averaging for model merging. *arXiv preprint arXiv:2412.12153*, 2024. 2, 3, 5
- [7] Mircea Cimpoi, Subhransu Maji, Iasonas Kokkinos, Sammy Mohamed, and Andrea Vedaldi. Describing textures in the wild. In *CVPR*, pages 3606–3613, 2014. 5, 1
- [8] Karl Cobbe, Vineet Kosaraju, Mohammad Bavarian, Mark Chen, Heewoo Jun, Lukasz Kaiser, Matthias Plappert, Jerry Tworek, Jacob Hilton, Reiichiro Nakano, et al. Training verifiers to solve math word problems. *arXiv preprint arXiv:2110.14168*, 2021. 5, 1
- [9] Tianshuo Cong, Delong Ran, Zesen Liu, Xinlei He, Jinyuan Liu, Yichen Gong, Qi Li, Anyu Wang, and Xiaoyun Wang. Have you merged my model? on the robustness of large language model ip protection methods against model merging. In *Proceedings of the 1st ACM Workshop on Large AI Systems and Models with Privacy and Safety Analysis*, pages 69–76, 2023. 1
- [10] Pala Tej Deep, Rishabh Bhardwaj, and Soujanya Poria. Della-merging: Reducing interference in model merging through magnitude-based sampling. *arXiv preprint arXiv:2406.11617*, 2024. 2, 3, 5
- [11] Alexey Dosovitskiy. An image is worth 16x16 words: Transformers for image recognition at scale. *arXiv preprint arXiv:2010.11929*, 2020. 1, 5
- [12] Guodong Du, Junlin Lee, Jing Li, Runhua Jiang, Yifei Guo, Shuyang Yu, Hanting Liu, Sim K Goh, Ho-Kin Tang, Daojing He, et al. Parameter competition balancing for model merging. *NeurIPS*, 37:84746–84776, 2024. 2, 3, 5
- [13] GitHub. Github repository. <https://github.com>, 2025. Accessed: 2025-11-12. 1
- [14] Patrick Helber, Benjamin Bischke, Andreas Dengel, and Damian Borth. Eurosat: A novel dataset and deep learning benchmark for land use and land cover classification. *IEEE Journal of Selected Topics in Applied Earth Observations and Remote Sensing*, 12(7):2217–2226, 2019. 5, 1
- [15] Geoffrey Hinton, Oriol Vinyals, and Jeff Dean. Distilling the knowledge in a neural network. *arXiv preprint arXiv:1503.02531*, 2015. 3
- [16] Gabriel Ilharco, Marco Tulio Ribeiro, Mitchell Wortsman, Ludwig Schmidt, Hannaneh Hajishirzi, and Ali Farhadi. Editing models with task arithmetic. In *ICLR*, 2023. 1, 2, 3, 5, 6
- [17] Albert Q. Jiang, Alexandre Sablayrolles, Arthur Mensch, Chris Bamford, Devendra Singh Chaplot, Diego de las Casas, Florian Bressand, Gianna Lengyel, Guillaume Lample, Lucile Saulnier, L elio Renard Lavaud, Marie-Anne Lachaux, Pierre Stock, Teven Le Scao, Thibaut Lavril, Thomas Wang, Timoth ee Lacroix, and William El Sayed. Mistral 7b, 2023. 5
- [18] Wei Junhao, Yu Zhe, and Jun Sakuma. Disrupting model merging: A parameter-level defense without sacrificing accuracy. In *ICCV*, pages 17698–17707, 2025. 1, 2, 5, 6
- [19] Jonathan Krause, Michael Stark, Jia Deng, and Li Fei-Fei. 3d object representations for fine-grained categorization. In *ICCV Workshops*, pages 554–561, 2013. 5, 1
- [20] Yann LeCun. The mnist database of handwritten digits. <http://yann.lecun.com/exdb/mnist/>, 1998. 5, 1
- [21] Dongfang Li, Zetian Sun, Xinshuo Hu, Zhenyu Liu, Ziyang Chen, Baotian Hu, Aiguo Wu, and Min Zhang. A survey of large language models attribution. *arXiv preprint arXiv:2311.03731*, 2023. 1
- [22] Hao Li, Zheng Xu, Gavin Taylor, Christoph Studer, and Tom Goldstein. Visualizing the loss landscape of neural nets. *NeurIPS*, 31, 2018. 4, 8
- [23] Xuechen Li, Tianyi Zhang, Yann Dubois, Rohan Taori, Ishaan Gulrajani, Carlos Guestrin, Percy Liang, and Tatsunori B Hashimoto. AlpacaEval: An automatic evaluator of instruction-following models, 2023. 5, 1
- [24] Zhenyi Lu, Chenghao Fan, Wei Wei, Xiaoye Qu, Danyang Chen, and Yu Cheng. Twin-merging: Dynamic integration of modular expertise in model merging. *NeurIPS*, 37:78905–78935, 2024. 2, 3, 5
- [25] ModeScope. Modelscope: Open-source model platform. <https://modelscope.cn/>, 2025. Accessed: 2025-11-12. 1
- [26] Yuval Netzer, Tao Wang, Adam Coates, Alessandro Bissacco, Baolin Wu, Andrew Y Ng, et al. Reading digits in natural images with unsupervised feature learning. In *NeurIPS Workshop on deep learning and unsupervised feature learning*, page 7. Granada, 2011. 5, 1
- [27] Binhang Qi, Hailong Sun, Wenrui Long, Ruobing Zhao, Xiang Gao, et al. Cabs: Conflict-aware and balanced sparsification for enhancing model merging. In *ICML*, 2025. 1
- [28] Alec Radford, Jong Wook Kim, Chris Hallacy, Aditya Ramesh, Gabriel Goh, Sandhini Agarwal, Girish Sastry, Amanda Askell, Pamela Mishkin, Jack Clark, et al. Learning transferable visual models from natural language supervision. In *ICML*, pages 8748–8763. PMLR, 2021. 1
- [29] Robin Rombach, Andreas Blattmann, Dominik Lorenz, Patrick Esser, and Bj orn Ommer. High-resolution image synthesis with latent diffusion models. In *CVPR*, pages 10684–10695, 2022. 5

- [30] Johannes Stalkamp, Marc Schlipf, Jan Salmen, and Christian Igel. The german traffic sign recognition benchmark: a multi-class classification competition. In *IJCNN*, pages 1453–1460. IEEE, 2011. 5, 1
- [31] Derek Tam, Mohit Bansal, and Colin Raffel. Merging by matching models in task parameter subspaces. *Transactions on Machine Learning Research (TMLR)*, 2024. 4
- [32] Gemma Team, Morgane Riviere, Shreya Pathak, Pier Giuseppe Sessa, Cassidy Hardin, Surya Bhupatiraju, Léonard Hussenot, Thomas Mesnard, Bobak Shahriari, Alexandre Ramé, et al. Gemma 2: Improving open language models at a practical size. *arXiv preprint arXiv:2408.00118*, 2024. 5
- [33] Hugo Touvron, Louis Martin, Kevin Stone, Peter Albert, Amjad Almahairi, Yasmine Babaei, Nikolay Bashlykov, Soumya Batra, Prajjwal Bhargava, Shruti Bhosale, et al. Llama 2: Open foundation and fine-tuned chat models. *arXiv preprint arXiv:2307.09288*, 2023. 1, 5
- [34] Lewis Tunstall, Edward Emanuel Beeching, Nathan Lambert, Nazneen Rajani, Kashif Rasul, Younes Belkada, Shengyi Huang, Leandro Von Werra, Clémentine Fourrier, Nathan Habib, et al. Zephyr: Direct distillation of lm alignment. In *COLM*, 2024. 5
- [35] Lixu Wang, Shichao Xu, Ruiqi Xu, Xiao Wang, and Qi Zhu. Non-transferable learning: A new approach for model ownership verification and applicability authorization. In *ICLR*, 2022. 1
- [36] Tianyu Wang, Jianzong Wang, Shiliang Zhang, and Jing Xiao. A survey of knowledge distillation: Techniques, applications and outlook. *IEEE Trans. Neural Networks and Learning Systems.*, 34(3):1231–1249, 2023. 3
- [37] Yongxian Wei, Anke Tang, Li Shen, Chun Yuan, and Xiaochun Cao. Modeling multi-task model merging as adaptive projective gradient descent. In *ICML*, 2025. 4
- [38] WikiArts. Wikiarts captions. https://huggingface.co/datasets/fusing/wikiart_captions, 2025. Accessed: 2025-11-12. 5, 1
- [39] Thomas Wolf, Lysandre Debut, Victor Sanh, Julien Chaumond, Clement Delangue, Anthony Moi, Pierric Cistac, Tim Rault, Rémi Louf, Morgan Funtowicz, et al. Huggingface’s transformers: State-of-the-art natural language processing. *arXiv preprint arXiv:1910.03771*, 2019. 1
- [40] Mitchell Wortsman, Gabriel Ilharco, Samir Ya Gadre, Rebecca Roelofs, Raphael Gontijo-Lopes, Ari S Morcos, Hongseok Namkoong, Ali Farhadi, Yair Carmon, Simon Kornblith, et al. Model soups: averaging weights of multiple fine-tuned models improves accuracy without increasing inference time. In *ICML*, pages 23965–23998. PMLR, 2022. 1, 2, 3, 5, 6
- [41] Jianxiong Xiao, James Hays, Krista A Ehinger, Aude Oliva, and Antonio Torralba. Sun database: Large-scale scene recognition from abbey to zoo. In *CVPR*, pages 3485–3492. IEEE, 2010. 5, 1
- [42] Prateek Yadav, Derek Tam, Leshem Choshen, Colin A Raffel, and Mohit Bansal. Ties-merging: Resolving interference when merging models. *NeurIPS*, 36:7093–7115, 2023. 1, 2, 3, 5, 6
- [43] Shojiro Yamabe, Futa Kai Waseda, Tsubasa Takahashi, and Koki Wataoka. MergePrint: Merge-resistant fingerprints for robust black-box ownership verification of large language models. In *Proceedings of the 63rd Annual Meeting of the Association for Computational Linguistics (Volume 1: Long Papers)*, pages 6894–6916. Association for Computational Linguistics, 2025. 1
- [44] Enneng Yang, Li Shen, Guibing Guo, Xingwei Wang, Xiaochun Cao, Jie Zhang, and Dacheng Tao. Model merging in llms, mllms, and beyond: Methods, theories, applications and opportunities. *arXiv preprint arXiv:2408.07666*, 2024. 1
- [45] Enneng Yang, Li Shen, Zhenyi Wang, Guibing Guo, Xiaojun Chen, Xingwei Wang, and Dacheng Tao. Representation surgery for multi-task model merging. In *ICML*, pages 56332–56356, 2024. 1
- [46] Enneng Yang, Zhenyi Wang, Li Shen, Shiwei Liu, Guibing Guo, Xingwei Wang, and Dacheng Tao. Adamerging: Adaptive model merging for multi-task learning. In *ICLR*, 2024. 2, 3, 5, 6
- [47] Yan Yang, Yixia Li, Hongru Wang, Xuetao Wei, James Jianqiao Yu, Yun Chen, and Guanhua Chen. Impart: Importance-aware delta-sparsification for improved model compression and merging in llms. In *Proceedings of the 63rd Annual Meeting of the Association for Computational Linguistics (Volume 1: Long Papers)*, pages 18817–18829, 2025. 1
- [48] Le Yu, Bowen Yu, Haiyang Yu, Fei Huang, and Yongbin Li. Language models are super mario: Absorbing abilities from homologous models as a free lunch. In *ICML*, 2024. 1, 2, 5
- [49] Luca Zhou, Daniele Solombrino, Donato Crisostomi, Maria Sofia Bucarelli, Giuseppe Alessio D’Inverno, Fabrizio Silvestri, and Emanuele Rodolà. On task vectors and gradients. *arXiv preprint arXiv:2508.16082*, 2025. 4

Defending Unauthorized Model Merging via Dual-Stage Weight Protection

Supplementary Material

The content of Supplementary Material is summarized as follows: 1) In Sec. A, we introduce the dataset used in our experiments across the vision and language domains; 2) In Sec. B, we describe the Transformer-based model architecture, focusing on the MLP and multi-head attention modules; 3) In Sec. C, we report the time cost of mask evaluation in MERGEGUARD; 4) In Sec. D, we provide additional results, including image and code generation, which offer further evidence of the effectiveness of MERGEGUARD.

A. Experimental Details

A.1. Environments

All experiments in this paper were conducted on a system with an Intel Core i9-10900X CPU and four NVIDIA RTX 3090 GPUs. The LLM experiments were executed on two NVIDIA H100 GPUs. The operating system was Ubuntu 18.04.6 LTS, and all software and dependencies were run in a Python 3.10 environment.

A.2. Datasets Details

Image Classification. We summarize the datasets used in our experiments in Table 6, including the number of classes, training samples, and test samples for each. These datasets [5, 7, 14, 19, 20, 26, 30, 41] are standard benchmarks for evaluating model merging in image classification tasks.

Image Generation. We use a diffusion model finetuned on the WikiArt dataset [38] and the Naruto dataset [2]. WikiArt contains high-resolution paintings curated across diverse artistic genres such as Impressionism, Realism, and Abstract Art, which makes it suitable for assessing stylistic fidelity, texture quality, and semantic consistency. Naruto provides a high-quality collection of anime frames and character-centered scenes and is widely used to evaluate generative models on non-photorealistic, domain-specific visual distributions.

LLM Evaluation. We employ three language datasets [4, 8, 23] to evaluate the capability of LLMs, including instruction following, mathematical reasoning, and program synthesis.

- AlpacaEval [23] is a benchmark designed to evaluate instruction-following ability in large language models. It contains approximately 805 human-authored instructions that span diverse open-ended tasks such as reasoning, explanation, transformation, and multi-step guidance. Model responses are compared against strong reference answers through pairwise preference scoring, which provides a reliable measure of general instruction alignment in generative models.

- GSM8K [8] is a high-quality dataset of grade-school mathematical word problems that require multi-step quantitative reasoning, arithmetic manipulation, and logical deduction. It contains 8,792 problems in total, with 7,473 examples for training and 1,319 for testing. Each problem includes a detailed step-by-step solution, making GSM8K a widely used and reliable benchmark for evaluating mathematical reasoning in language models.
- HumanEval [4] is a dataset of 164 hand-written Python programming problems paired with unit tests. Each prompt requires generating a function that satisfies the specified behavior, and functional correctness is evaluated by checking whether the model-generated code passes all provided test cases. This benchmark is widely used to assess program synthesis and code generation capabilities.

B. Model Architecture

Our method is tailored to Transformer-based architectures, where each layer, or Transformer block, consists of a multi-head attention submodule and a multilayer perceptron (MLP). This architecture serves as the foundation of many modern deep learning models, including ViT, Stable Diffusion models, and LLMs. Because our method closely interacts with the structure of both the attention and MLP submodules, we outline their roles and computations within a typical Transformer block.

MLP. The MLP submodule applies nonlinear transformations to each position’s feature vector, often scaling dimensions in the hidden layer. Given a feature vector $X \in \mathbb{R}^d$ at a single spatial or temporal position, a standard two-layer MLP computes

$$\text{MLP}(X) = W_2\sigma(W_1X + b_1) + b_2,$$

where $W_1 \in \mathbb{R}^{h \times d}$, $W_2 \in \mathbb{R}^{d \times h}$ are the learned weight matrices, b_1, b_2 are the corresponding biases, and $\sigma(\cdot)$ denotes a nonlinear activation such as GELU. Because the computation is applied independently to each token, the MLP enriches the representation capacity of the Transformer block without introducing interactions across positions.

Structure of Multi-head Attention Block. Consider a multi-head attention module with h heads, each operating on vectors of dimensionality d_k . Let the input sequence be $x \in \mathbb{R}^{seq \times d_{model}}$. A learned linear projection maps this sequence into combined query, key, and value matrices, $Q, K, V \in \mathbb{R}^{seq \times (h \times d_k)}$. These matrices are then partitioned along the

Table 6. Dataset descriptions used in our image classification experiments.

Attribute	SUN397	Cars	RESISC45	EuroSAT	SVHN	GTSRB	MNIST	DTD
Domain	Scene recognition	Fine-grained car models	Remote sensing scenes	Satellite imagery	Digits in natural scenes	Traffic signs	Handwritten digits	Texture recognition
#Classes	397	196	45	10	10	43	10	47
Train Images	76,128	8,144	24,300	21,600	73,257	39,209	60,000	3,760
Test Images	32,626	8,041	7,200	5,400	26,032	12,630	10,000	1,880
Resolution	256×256	224×224	256×256	64×64	32×32	32×32	28×28	224×224

feature dimension into h groups:

$$\begin{aligned} Q &\rightarrow \{Q_1, \dots, Q_h\}, \\ K &\rightarrow \{K_1, \dots, K_h\}, \\ V &\rightarrow \{V_1, \dots, V_h\}, \end{aligned}$$

where each $Q_i, K_i, V_i \in \mathbb{R}^{seq \times d_k}$ serves as the input to the i -th attention head. For each head, the attention computation is

$$\text{Attn}(Q_i, K_i, V_i) = \text{Softmax}\left(\frac{Q_i K_i^T}{\sqrt{d_k}}\right) V_i.$$

After all heads produce their outputs, the resulting vectors are concatenated and transformed through an output projection. Equivalently, the final attention representation can be written as

$$\text{Attention}(Q, K, V) = \sum_{i=1}^h \text{Attn}(Q_i, K_i, V_i) W_{\text{out}}^{(i)},$$

where $W_{\text{out}}^{(i)} \in \mathbb{R}^{d_k \times d_{\text{model}}}$ denotes the corresponding block of the output projection matrix.

C. Time Cost of Mask Evaluation

We calculate the evaluation time (in minutes) for the mask in the second stage. As shown in Table 7 and Table 8, the evaluation time increases with the size of the dataset, indicating that mask computation becomes more costly as more task-relevant samples are processed. This occurs because MERGE GUARD must identify and preserve task-critical weights, prevent the removal of important parameters during subsequent weight suppression, and maintain model accuracy after merging. We regard this time cost as acceptable since it meaningfully reduces the risk posed by potential free riders.

Table 7. Time cost (mins) of ViT-L-14 across various datasets.

SUN397	Cars	RESISC45	EuroSAT
557.28	278.64	130.75	174.02
SVHN	GTSRB	MNIST	DTD
371.52	128.71	108.00	51.60

Table 8. Time cost (mins) of different LLMs across various tasks.

Task	Llama2	Gemma2	Mistral	Avg.
Instruction (AlpacaEval)	641.20	512.12	358.41	503.91
Math (GSM8K)	606.50	451.58	293.08	450.39
Code (HumanEval)	404.30	330.78	312.65	349.24

D. Additional Results

D.1. Visualization Results on SD1.5

Figure 5 presents additional results of MERGE GUARD on image generation tasks. We use Animate as the defender’s task (T_{def}) and “The Simpsons” as the free-rider’s task (T_{fr}). The first two columns show the images generated by θ_{def} and θ_{fr} , respectively. When tested with the prompts C_0 and C_1 designed for Animate, the free-rider’s model θ_{fr} is also able to reproduce the character, indicating that it has captured the semantic style of Animate. The merged model θ_{merge} , obtained through standard parameter fusion, inherits this ability and successfully generates Animate-style images, which demonstrates a clear instance of intellectual property leakage. In contrast, MERGE GUARD preserves the performance of $\hat{\theta}_{\text{def}}$ while effectively degrading the quality of $\hat{\theta}_{\text{merge}}$, preventing the free-rider from reproducing Animate-style content.

D.2. Code Results

We further report the results on code generation using HumanEval. MERGE GUARD effectively suppresses the performance of the merged model, often reducing it by more than half. We also observe that many generated programs, even when producing a passing result, contain substantial redundant code, unnecessary library imports, or code that leads to infinite loops. Figure 6 provides an example in which the generated program repeatedly produces the same invalid output. The results validate that MERGE GUARD reliably degrades merged model performance and prevents the generation of valid programs.



Figure 5. Visualization of images generated using SD1.5. The left panel displays an example prompt, and the right panel shows the corresponding outputs from each model.

```
def truncate_number_to_n_decimals_with_commas_and_space(number: float, n: int) -> str:
    """ Given a positive floating point number, it can be decomposed into
    and integer part (largest integer smaller than given number) and decimals
    (leftover part always smaller than 1).

    Return the decimal part of the number truncated to n decimals.
    >>> truncate_number_to_n_decimals_with_commas_and_space(3.5, 1)
    '0,5 '
    >>> truncate_number_to_n_decimals_wth_commas_and_space(3.5, 2)
    '0,50 '
    """
    return truncate_number_to_n_decimals_with_commas(number, n) + ' '

def truncate_number_to_n_decimals_with_commas_and_space_and_percent(number: float, n: int) -> str:
    """ Given a positive floating point number, it can be decomposed into
    and integer part (largest integer smaller than given number) and decimals
    (leftover part always smaller than 1).

    Return the decimal part of the number truncated to n decimals.
    >>> truncate_number_to_n_decimals_with_commas_and_space_and_percent(3.5, 1)
    '0,5 %'
    >>> truncate_number_to_n_decimals_wth_commas_and_space_and_percent(3.5, 2)
    '0,50 %'
    """
    return truncate_number_to_n_decimals_with_commas_and_space(number, n) + '% '

def truncate_number_to_n_decimals_with_commas_and_space_and_percent_and_space(number: float, n: int) -> str:
    """ Given a positive floating point number, it can be decomposed into
    and integer part (largest integer smaller than given number) and decimals
    (leftover part always smaller than 1).

    Return the decimal part of the number truncated to n decimals.
    >>> truncate_number_to_n_decimals_with_commas_and_space_and_percent_and_space(3.5, 1)
    '0,5 % '
    >>> truncate_number_to_n_decimals_wth_commas_and_space_and_percent_and_space(3.5, 2)
    '0,50 % '
    """
    return truncate_number_to_n_decimals_with_commas_and_space_and_percent(number, n) + '% '

```

Figure 6. Redundant or looping code generated by the merged model protected with MERGE GUARD.